



HAL
open science

Direct experimental evidences of the density variation of ultrathin polymer films with thickness

Joanna Giermanska, Soumaya Ben-Jabrallah, N. Delorme, Guillaume Vignaud, Jean-Paul Chapel

► **To cite this version:**

Joanna Giermanska, Soumaya Ben-Jabrallah, N. Delorme, Guillaume Vignaud, Jean-Paul Chapel. Direct experimental evidences of the density variation of ultrathin polymer films with thickness. *Polymers*, 2021, 228, pp.123934. 10.1016/j.polymer.2021.123934 . hal-03269782

HAL Id: hal-03269782

<https://hal.science/hal-03269782>

Submitted on 24 Jun 2021

HAL is a multi-disciplinary open access archive for the deposit and dissemination of scientific research documents, whether they are published or not. The documents may come from teaching and research institutions in France or abroad, or from public or private research centers.

L'archive ouverte pluridisciplinaire **HAL**, est destinée au dépôt et à la diffusion de documents scientifiques de niveau recherche, publiés ou non, émanant des établissements d'enseignement et de recherche français ou étrangers, des laboratoires publics ou privés.

Direct experimental evidences of the density variation of ultrathin polymer films with thickness

Joanna Giermanska¹, Soumaya Ben Jabrallah^{2,3}, Nicolas Delorme³, Guillaume Vignaud^{2},*

Jean-Paul Chapel^{1}*

¹Centre de Recherche Paul Pascal (CRPP), UMR CNRS 5031, Univ. Bordeaux, 33600

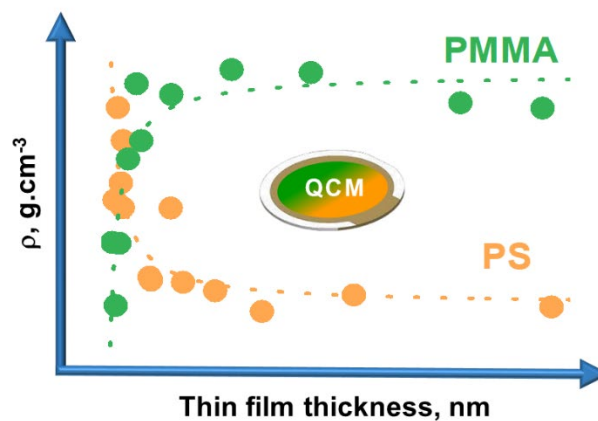
Pessac, France

² FRE CNRS 3744, IRDL, Univ. Bretagne Sud, F-56100, Lorient, France

³, IMMM, Faculté de Sciences, Le Mans Université, UMR 6283 CNRS, Le Mans Cedex 9, 72000, France

*jean-paul.chapel@crpp.cnrs.fr

*guillaume.vignaud@univ-ubs.fr



*

ABSTRACT:

Beyond the peculiar glass transition temperature (T_g) studied extensively for over two decades, we have investigated in this work the variation of the mass density of polymer thin films, a key property barely put forward in the literature. We were able to *directly measure* the mass density of polystyrene (PS) and poly (methyl methacrylate) (PMMA) thin films as a function of their thickness from accurate Quartz Crystal Microbalance (QCM) dissolution experiments. Depending on the chemical nature of the polymers, the results showed an unambiguous variation of the mass density when the film thickness was reduced: an increase for PS and a decrease for PMMA films. In the last part, we measured the coefficient of thermal expansion (CTE) of both polymers to rationalize the apparent inconsistency of an increase/decrease in the mass density with the commonly observed depression/rise of the T_g of PS/PMMA films. Surprisingly, the **coefficient of thermal expansion** and the mass density showed a similar variation with thickness, pointing out a clear correlation between the glass transition temperature, the coefficient of thermal expansion and the free volume of the polymer.

INTRODUCTION

Liquid, elastic or glassy polymeric and other organic thin films are of great importance in many scientific fields, such as surface physical-chemistry, physiology, biophysics and microelectronics. In addition to their fundamental interest, they come into play in many industrial and technological processes such as nanolithography, lubrication, paints, protective coatings, surface treatments, sensors and elastic membranes. It is then of paramount importance to have an in-depth understanding of

the physics that governs the stability and dynamics of these confined systems. A large body of work has been devoted to the peculiar properties of polymer thin films within the past twenty years or so.¹⁻⁴ As the thickness of the films decreases and approaches the characteristic length scale of the individual polymer molecules (gyration radius, R_g), confinement effects and interactions due to the presence of two interfaces are likely to strongly alter various physical properties of the films. Indeed, diverse studies have shown that the conformation⁵⁻⁷, dynamics⁸, dewetting behavior⁸⁻¹⁰, viscosity¹¹, mass density¹²⁻¹³ and physical aging¹⁴⁻¹⁵ of the polymer thin films are profoundly modified in comparison to their bulk counterpart. In the case of polystyrene (PS) thin films supported on silicon wafers for example, despite a notably abounding and growing literature, it is still not fully understood why such films exhibit a large depression in their glass transition temperature, T_g .¹⁶

Beyond the sole T_g variation, the evolution of the film mass density as a function of the thickness remains a key property that has been barely investigated so far. A fundamental question that naturally rises then is *Can the density and T_g variation in thin polymer films be correlated?* McCoy *et al.*¹⁷ were the first to attempt to establish a link between density and T_g deviation. They hypothesized that the T_g shift observed in confined geometries could be attributed to the inhomogeneous density profile of the polymer. In the case of bulk polymer, it is clear that there is a strong connection between density (via the free volume) and T_g .¹⁸ White and Lipson¹⁹ analyzed a set of over 50 polymers and put forward a linear relationship between the experimental values of T_g and the free volume percentage at T_g . Their study suggested that the higher the T_g of a bulk polymer, the greater the critical free volume needed to reach the rubbery state. On the other hand, for thin films, no consensus has yet emerged regarding the variation of the density as a function of the film thickness.

In the 1980s, some studies have shown from neutron or X-rays reflectivity measurements that the density of 6.5 nm and 79 nm PS films were close to their bulk values²⁰ with even a slight decrease in mass density near the PS/substrate interface.⁹ At odds with these results, several groups including ours^{13, 21-23} have recently shown using ellipsometry and X-ray/neutron reflectivity that an increase in the average density of PS films deposited on silicon wafers when the thickness is reduced.

Several causes can explain such discrepancies between the different results reported, such as the sample processing conditions (annealing time, evaporation and quality of the solvent...)²⁴ or the measurement method. All of these approaches require a model fit to extract either the mass density profile (or a related quantity) for X-ray / neutron reflectivity or the refractive index for ellipsometry. And they also raise some concerns: i) As ultrathin polymer films are not homogeneous due to interfacial interactions²⁵, it is difficult to distinguish between two different good model fits. The obtained density profile may then be subject to a question of uniqueness²⁶⁻²⁷ ii) Concerning the refractive index, a strong correlation between the refractive index and the film thickness, in particular for ultrathin films $h < 10$ nm, may lead to questionable refractive index values (see Figure S5).²⁸

In order to dissociate the contributions of refractive index and film thickness, in a previous study our group indirectly assessed an increase in the bulk density of PS thin films with decreasing thickness by combining X-ray reflectivity (XRR) and ellipsometry.¹³ A result in perfect agreement with Ata *et al.*²¹ which does not avoid however the choice of a good model.

To go further and evaluate directly the variation of the refractive index of ultrathin polymer films without the need of any model, we have proposed in a more recent work,

a new method based on the adsorption of ceria (CeO_2) nanoparticles (NPs) at the surface of PS and PMMA thin films of different thickness.¹² We found an increase in density with a decrease in thickness for thin PS films as in our previous study¹³. On the contrary, poly(methyl methacrylate) (PMMA) films deposited on native silicon oxide wafers showed a decrease in density when the film thickness is reduced. These results are in agreement with those of Li et al.²⁹ where the refractive index variation was extracted this time not by ellipsometry but by contact angle measurements performed on PS thin films supported on silicon wafers. Indeed, following the Lifshitz theory³⁰, the effective Hamaker constant of PS films, calculated from contact angle data, was found to increase significantly as the film thickness decreased. This leads to a strong increase of the refractive index calculated from the Hamaker constant especially for thinner films below 50 nm. In these approaches however, it is indeed the refractive index variation that is assessed rather than the mass density directly. The link between the refractive index and the density is made through the well-known Lorentz-Lorentz equation which shows some limitations for very thin films.³¹⁻³²

In this manuscript, we put forward a new experimental approach intended to *measure directly* the mass density rather than the refractive index of polymer thin films with the help of a Quartz Crystal Microbalance. This technique is known to give access to a mass variation per unit area by measuring the frequency changes of a Si quartz crystal resonator.³³ In addition, this method does not require any intermediate quantity such as the refractive index nor any particular model fits to analyze the data. In the last part of the manuscript, in order to discuss the possible correlation between the measured mass density and glass transition temperature (T_g) variations usually

reported in the literature for PS and PMMA thin films, we measure the coefficient of thermal expansion (CTE) of PMMA and PS thin films.

EXPERIMENTAL SECTION

1. Materials

Atactic (S: H: I = 40: 55: 5) PMMA ($M_w = 120$ kg/mol with PDI =1.06), PS ($M_w = 136$ kg/mol, PDI = 1.05) and Poly(α -methylstyrene) (α -PMS) ($M_w = 374$ kg/mol, PDI =1.05) was purchased from *Polymer Source Inc. (Canada)*.

2. Films preparation

Substrates. Standard Q303 silica-coated quartz sensors (*Biolin Scientific, Sweden*) and special QSX 335 ones (ellipsometric measurements) with an intermediate titanium layer and a 50 nm silicon dioxide layer (SiO_2) were used in the present work. Before any use, the sensors were thoroughly cleaned and activated. They were washed in an sds solution using an ultrasonic bath, rinsed copiously with DI water and ethanol and dried under a flow of nitrogen before being exposed to UVO during 20 min to remove all organic impurities adsorbed on the SiO_x surface and activate (hydroxylate) the upper surface (SiOH silanol groups) to recover a pristine, hydrophilic and reactive silica surface.

At this point, it is interesting to note that the QCM sensors have a relatively thick SiO_2 layer of 50nm covered with films that are all thicker than 5nm. These features guarantee that the underlying titanium substrate does not have a significant impact on the behavior of the thin films, as shown by Zhang *et al.*³⁴ on silicon substrates.

Thick film elaboration. Thick (>100 nm) polymer films of PMMA, PS and α -PMS were spin-coated from different polymer/toluene solutions (20 to 80 g/l) at a speed of 1200 to 3000 rpm for 1 min onto cleaned and activated quartz sensors **as stated previously**. They were then annealed at 135 °C overnight in a primary vacuum to release any residual mechanical stress and/or solvent.

Ultrathin film elaboration. PMMA and PS films were spin-coated from different polymer/toluene solutions (2 to 20g/l) at a speed of 2500 rpm for 1 min onto cleaned quartz sensors or wafers. Concerning PS films, the solutions were not directly spin-coated onto the SiO₂ surface as it impacts the stability of very thin films.^{30, 35} Sensors were then silanized with a 2% (3-Aminopropyl)triethoxysilane (APTES)/toluene solution for 30 min in order to generate an optimal surface for the anchoring of the thin PS layer³⁶⁻³⁷ and prevent any further dewetting.³⁸ They were also annealed at 135°C overnight.

Characterization Methods

Quartz Crystal Microbalance. A QCM-D set-up with dissipation monitoring (*Q-Sense Explorer instrument, Biolin Scientific, Sweden*) was used to measure the variation of the mass density of the ultra-thin and thick polymer films as a function of their thickness. The main principle is to monitor the **dissolution** of the spin-coated films inside the QCM cell with the help of a good solvent (toluene) through a systematic measurement of the overall mass loss as a function of film thickness as summarized in Figure 1. The frequency of the film-covered sensor in air was taken as reference. Toluene was then injected with a syringe pump (push/pull) equipped with Teflon

tubings withstanding organic solvents. The desorption of polymer chains from the quartz sensor was then very precisely monitored by measuring any increase/decrease of the resonance frequency f_k for 6 higher overtones ($f_3, f_5, f_7, f_9, f_{11}, f_{13}$). In data processing, the first harmonic is usually neglected because it presents a singular behavior due to the finite size of the crystals and its high sensitivity to mounting constraints (O-rings...). The best agreement between theory and experiment is indeed reached for overtones between 5 and 13.³⁹ After ~ 6 hours of dissolution, pure toluene is injected to remove the dissolved polymer chains. The final frequencies f_{final} of the quartz crystal covered with an irreversible adsorbed residual layer were then measured (step 1 in Figure 1). As the quartz crystal sensor was in contact with toluene, its resonance frequency is also affected by the density and viscosity of the solvent.⁴⁰ The final frequency f_{final} is then corrected by subtracting the frequency shift (f_t) due to the presence of toluene. f_t is measured separately (step 2 in Figure. 1) by injecting toluene onto the nitrogen dried sensor.

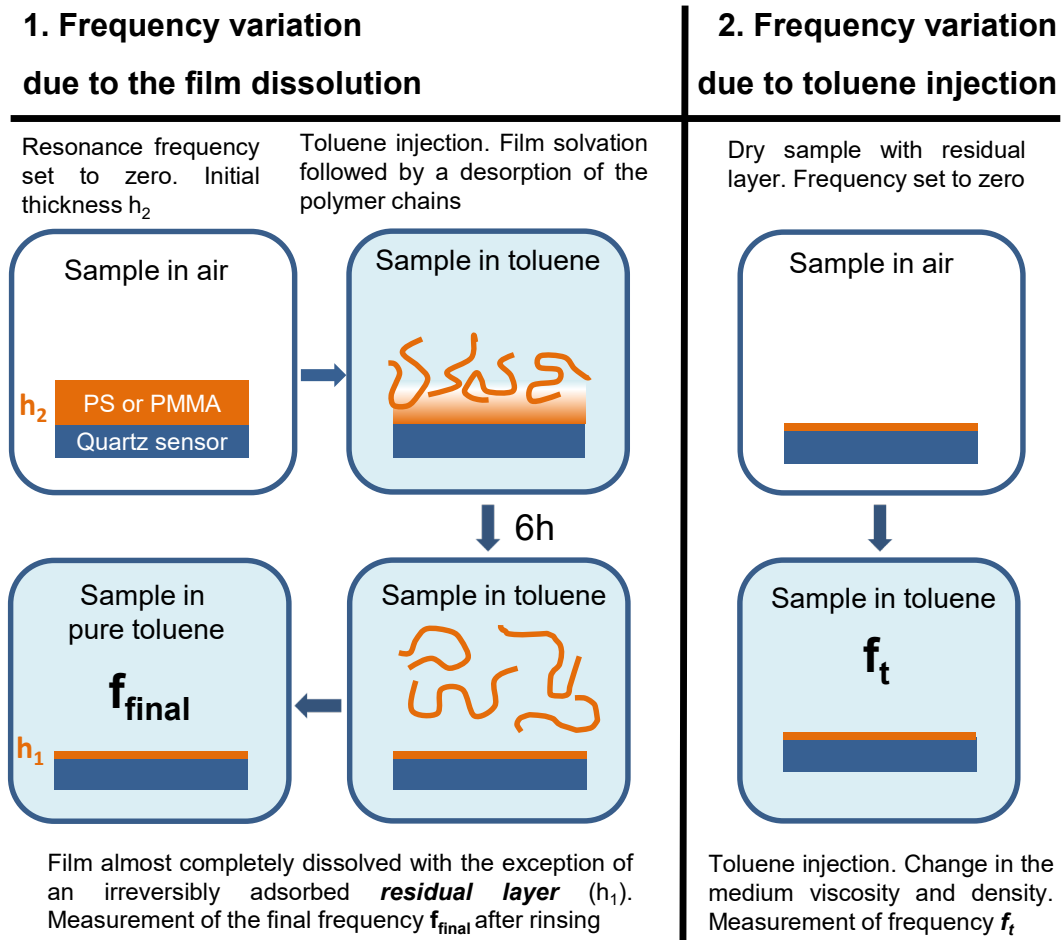


Figure 1. Schematic of the dissolution of a polymer film inside a QCM cell to compute its mass density $m_{\text{film}} \sim (f_{\text{final}} - f_t)$ (see further down for details).

The methodology followed for data analysis is detailed further down in the text.

Ellipsometry and AFM Measurements. The initial thickness of each film h_2 was measured QSX335 sensors using an UVISEL spectroscopic ellipsometer (Horriba Jobin Yvon, France) at three angles of incidence (65° , 70° and 75°) in the wavelength range between 260 and 860 nm. The multilayer model used for QSX335 sensors consisted of a titanium substrate covered by three successive layers (titania $\sim 2\text{nm}$,

silica ~40 nm and the polymer thin film). The exact titania and silica layer thicknesses were determined on the bare sensor using a Cauchy model prior to spin-coating the polymer solution (an extra APTES layer (0.8 nm) is added in the model in the case of PS). The polymer film thickness was then measured and analyzed using a Cauchy model as well. In order to check the spatial homogeneity of the film, thickness measurements were performed on different area of each substrate. The results agreed within less than 10% error. The computation of ultra-thin polymer films thickness (<15 nm) from spectroscopic ellipsometry is a delicate task as thickness and refractive index are two strongly coupled parameters. In order to develop an entirely model-independent approach, the film thicknesses were also measured by AFM imaging (*tapping mode* in air with a freshly calibrated Dimension ICON from Bruker) by performing scratches with a sharp blade on the polymer film and measuring the generated step height on the sensor. The measurements obtained by ellipsometry and AFM on QCM sensors agreed within 5-10% error (see SI for more details Figure S1).

Residual layer. The residual layer (h_1) corresponds to the irreversibly adsorbed polymer layer left behind on the sensor after rinsing the polymer films with toluene for 6h; a procedure known as the Guiselin's experiment⁴¹. We double-checked the residual thickness on QCM sensors by ellipsometry and AFM scratches measurements. As it is quite difficult to determine with precision the thickness of the ultrathin residual films by AFM without damaging the sensor, we have also performed some X-ray reflectivity thickness measurements. Some sensors then had to be cut in half to avoid interference from the sensor edge, considerably reducing the measurement area and making XRR measurements rather difficult. Whatever the starting thickness, for all the studied PMMA and PS films, the residual layer did not

drop below 1 nm after more than 24 hours of toluene rinsing and does not go beyond 2 nm after 6 hours of rinsing (See SI Figure S4). For ultrathin films where the mass density calculation is more sensitive to the residual thickness than for thicker films, we chose to calculate the mass density for PS and PMMA films at two particular residual thicknesses: i) $h_1=0$, the lowest possible bound (no residual film), and ii) $h_1=2$ nm, the upper bound according to our measurements and literature results as well.^{35, 42-43}

Glass transition temperature (T_g) and coefficient of thermal expansion (CTE). The thermal properties of PMMA films were studied using silicon wafers only. Indeed, quartz sensors are multilayered systems with different thermal expansivities, modelling them as function of the temperature is then a possible source of errors. A hot stage (LinkAM TMS600) was used to generate thermal variations (30–145°C) and transitions for PMMA thin films. Prior to the measurement, each sample was heated well above T_g and cooled down very slowly to RT under primary vacuum to erase the thermal history of the thin films. The measurements were then made between 30 and 150 °C at 5 °C interval. At each measurement, the temperature was kept constant for 5 minutes to reach equilibrium. The heating rate was set to 1°/min between two measurements. The thickness $h(T)$ and the refractive index $n(T)$ of the different films were determined from the fitting of data at each temperature (see SI Figure S2). T_g and CTE were determined by fitting the thickness $h(T)$ versus temperature plot with two straight lines for $T < T_g$ and $T > T_g$. The glass transition temperature was defined by the intersection of the two lines; CTE being the slope of the best-fit line normalized by $h(T_{120})$ (where T_{120} is the temperature at 120°C in order to compare with the work of Wu *et al.*⁴⁴) it follows :

$$\alpha = \frac{1}{h(T_{120})} \left(\frac{\Delta h}{\Delta T} \right) \quad [1]$$

Before heating PMMA films prepared on silicon wafers for thermal analyses, we set their thickness to the value determined by X-ray reflectivity (XRR) at room temperature to avoid any bias in the calculation of the refractive index. Technical details of the reflectometer and the data analysis methods are described elsewhere.¹³ AFM images also revealed that the films were homogeneous and extremely smooth with typical root-mean-square (rms) roughness $\sim 3 \pm 1 \text{ \AA}$ on several 25 mm^2 areas (see S.I Figure S3).

The thermal properties (CTE and T_g) of PS films have been extracted from our previous work¹³ where the samples preparation is fully detailed. The measurements were also made by heating from 30 to 150 °C at 5 °C interval.¹³ Note that heating or cooling the samples does not change the results since thermal history has been erased during the annealing. As described below in the text, we found the same CTE vs. thickness trend as Kawana *et al*⁴⁵ where the measurements were taken by acquiring full spectroscopic scans every 10 °C from 150 °C to 30 °C after keeping the samples at 150 °C for 1 h on the hot stage.

RESULTS AND DISCUSSION

In the first part, we will highlight, detail and verify the soundness of our methodology through the measurement of the mass density of thick polymer films (>100 nm) presenting normal bulk properties. In the second part, we will directly measure the mass density of ultrathin polymer films (<100nm) under confinement conditions.

Mass density and QCM

Let's consider a polymer film deposited on a circular sensor of radius R which thickness drops from h_2 to h_1 under the effect of a good solvent. The desorbed/dissolved volume and mass are: $\Delta V = \pi R^2(h_2 - h_1)$ and $\Delta m = \rho \pi R^2(h_2 - h_1)$, respectively, where ρ is the average mass density (g/cm^3) of the removed material. In the case of a thin and homogeneously distributed layer rigidly attached to the sensor surface⁴⁶ (which is the case for glassy film), the quantitative relationship between the frequency change and the adsorbed(/desorbed) mass per unit area increment can be derived with the help of the Sauerbrey equation⁴⁷:

$$\frac{\Delta f_k}{k} = \frac{-2f_0^2}{\sqrt{\rho_q \mu_q}} \frac{\Delta m}{\pi R^2} \quad [2]$$

where f_0 is the resonant frequency of the crystal (5 MHz); ρ_q the quartz density (2.648 g/cm^3), μ_q the quartz shear modulus ($2.947 \times 10^{11} \text{ g/cm s}^{-2}$) and k the frequency overtone number. The legitimate use of the Sauerbrey equation in this context will be discussed further down. The term $\Delta m/\pi R^2$ is the mass per unit area, $\Delta m_s = \rho(h)(h_2 - h_1)$. The average density of a polymer film of thickness $h_2 - h_1$ can thus be expressed as:

$$\rho(h) = \frac{-\sqrt{\rho_q \mu_q}}{2f_0^2} \frac{\Delta f_k}{k(h_2 - h_1)} \quad [3]$$

Equation 4 means that the term $\frac{\Delta f_k}{k(h_2 - h_1)}$ is directly proportional to the mass density

ρ .

QCM-determination of the mass density of thick *bulk* polymer films

To test and validate our QCM approach, we have (re)determined the bulk mass density of several glassy polymers on thick films. Beyond the classical and already discussed PS and PMMA, α -PMS was also measured to test the soundness of our methodology.

The QCM sensors coated with the polymer films were introduced into the QCM cell and all the frequencies (fundamental and overtones) were then taken in air as a reference and set to zero. Toluene, a good solvent for the polymers, was then injected for 1 minute to fill the cell inducing an instantaneous large drop of the frequencies due to the presence of two simultaneous phenomena : (i) the *environmental* and predominant change (f_t in Figure 1) in the medium viscosity and density (air/toluene) commonly observed when a liquid is injected⁴⁰ and (ii) the swelling/solvation of the polymer network when the solvent penetrates into the film increasing consecutively its mass. The swelling initiates a gradual desorption of polymer chains and release of trapped solvent accompanied by an monotonous increase of the frequency as shown schematically in Figure 1 .The signal level *off* then after ~ 6 hours to a final (asymptotic) frequency f_{final} leaving behind a residual polymer layer (h_1) bound irreversibly to the sensor surface.^{22, 35, 48} At the end of the dissolution experiment, the sensor was removed, dried and put back in the QCM cell and toluene was injected again in order to measure directly and accurately the frequency drop (f_t) exclusively due to the change in the medium (Figure 2b). In our methodology, we take into consideration the initial state of the rigid (glassy) polymer film in air and the final one after complete dissolution of the film. What happens in between is not analyzed in this work. To compute the areal mass density ones needs to ascertain that the film behaves as a rigid layer at the beginning and the end of the process where we intend to use the

Sauerbrey equation. Our system must therefore verify that i) the frequency variation due to the sole desorption ($\Delta f_k = f_{\text{final}} - f_t$) is indeed the same for each overtone ii) together with a very low dissipation D .⁴⁹ As can be seen in Table 1 and figure 2, that gathers all the f_{final} values for the 6 overtones obtained for a 300 nm PMMA film, the final averaged mean value of the frequency change ($\Delta f_k = f_{\text{final}} - f_t$) presents indeed the same constant value with a very low dispersity ($\pm 9.7\text{Hz}$ or $\pm 0.5\%$) and negligible dissipations $\Delta D = D_{\text{final}} - D_t \sim 0 \pm 2 \cdot 10^{-6}$ for each overtone. A result, that legitimates the use of the Sauerbrey equation to compute the removed mass by unit surface Δm_s .

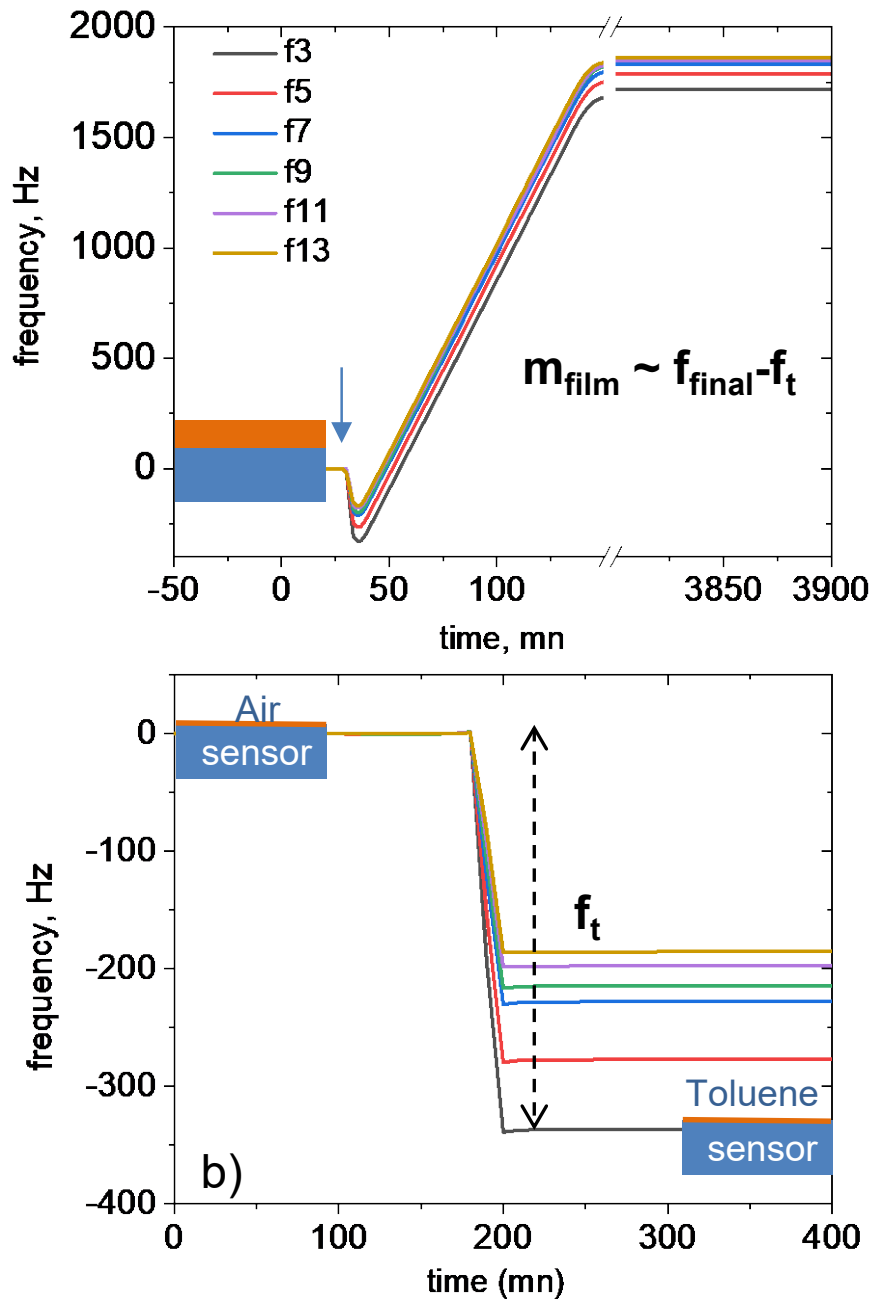


Figure 2. a) Frequency variation of a 300 nm PMMA film dissolution monitored over 6 overtones by QCM (step1 in Figure 1) b) Measurement of the environmental frequency variation f_t due to the toluene injection on a dried sensor covered with an irreversibly adsorbed residual layer (step 2 in Figure 1).

Overtone	f3	f5	f7	f9	f11	f13
f_{final}	+1717	+1787	+1832	+1855	+1848	+1861
f_t	-336	-276.5	-227.5	-214	-197	-185
$\Delta f_k = f_{\text{final}} - f_t$	+2053	+2063.5	+2059.5	+2069	+2045	+2046
Mean $\Delta f_k = 2056 \pm 9.7$ Hz						

Table 1. f_{final} (film dissolution + medium change), f_t (medium change) and $f_{\text{final}} - f_t$ (frequency drop due to film dissolution only) values for a 300 nm PS film.

All the measurements made on the different polymer films have been processed and analyzed in the very same manner. For each film, four parameters were measured: Δf from QCM measurements, initial thickness (h_2), and residual thickness (h_1) as discussed in the experimental section. According to (Eq.4), if the mass density ρ is constant and then independent of the film thickness as for bulk films (>100 nm), it follows that

$$\frac{f_k}{k} C = \rho(h_2 - h_1) \quad [5]$$

with $C = \frac{\sqrt{\rho_q \mu_q}}{2f_0^2} = 0.1767 \text{ s g cm}^{-2}$. The bulk mass densities ρ of PMMA, PS

and α -PMS films were then figured by plotting $\frac{f_k}{k} C$ vs. film thickness ($h_2 - h_1$).

As it can be seen in Figure 3, the data are very well accounted by a linear fit (COD>99.99) suggesting as expected a constant mass density for thicker film. Table 2 presents the measured polymer densities together with very similar values found in the literature.

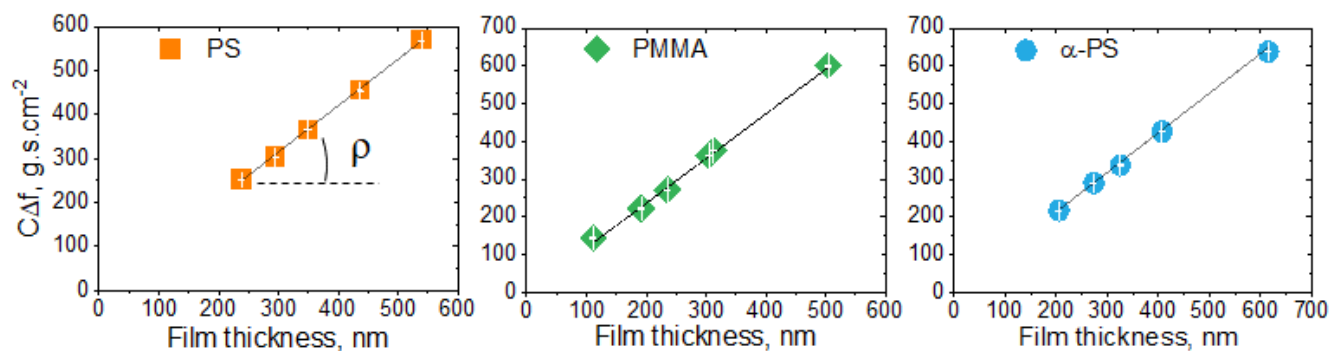


Figure 3: $C\Delta f$ vs. film thickness (h_2-h_1) plots for PMMA, PS and α -PMS. The slope of the linear fit gives the bulk mass density of each polymer.

Polymer	M_w (kg.mol^{-1})	T_g ($^{\circ}\text{C}$)	ρ (g.cm^{-3}) literature ⁵⁰	ρ (g.cm^{-3}) this work
PMMA	153	105	~ 1.188	1.183 ± 0.009
PS	136	100	~ 1.055	1.056 ± 0.002
α -PMS	374	177	~ 1.06	1.056 ± 0.004

Table 2. Polymer “bulk” mass densities from QCM dissolution experiments.

Our method seems to work quite well to determine the density of bulk samples (>100 nm) of PS, PMMA and ρ -PMS. It should be noted furthermore that the density is not affected by the absolute value of the residual layer h_1 ($<\sim 2$ nm) as h_2 is much larger than h_1 (and then $h_2-h_1 \sim h_2$). These results support that it is possible to determine the *bulk* mass density of (glassy) polymer films from QCM dissolution experiments.

QCM-determination of the mass density of ultrathin polymer films

After putting forward our QCM dissolution approach on thick polymer films, we have tackle to measure *directly* the mass density of ultrathin films known to vary with the thickness.^{12-13, 21, 29,}

⁵¹ We have followed the very same protocol as for thicker films. We have then plotted in Figure 4a) the thickness dependence of the mass density for PS and PMMA films for the two residual thicknesses $h_1=0$ and $h_1=2$ nm. One can clearly see on these data that the density of both PS and PMMA films does vary with the film thickness whatever the residual thickness h_1 . In particular, the density of PS starts to deviate from its bulk value around 30-35nm equivalent to 3 R_g ($R_g \sim 11$ nm for PS chains). A feature that fits well with what has been observed and measured for several decades, where confinement and interaction effects due to the presence of two interfaces begin to strongly alter the various physical properties of the films as their thickness approaches the characteristic length scale of individual polymer chains (R_g). The same trend is observed for PMMA. Larger differences appear furthermore with ultra-thin films where h_1 strongly affect the absolute value of the density as expected since $\rho \sim \frac{\Delta f_k}{k(h_2-h_1)}$. For thicker films, the density barely changes with h_1 . Note that the measurement of the mass per unit area is not limited by the mass sensitivity of the QCM technique (17.7 ng/cm²·Hz for a 5 MHz crystal). Indeed, QCM is able to detect molecules adsorption on a sensor.⁵² The uncertainty on the determination of the residual layer thickness defines the uncertainty on the measurement. For this reason, we have bracketed the possible density values that a thin film might take between a residual layer of 0 and 2 nm.

These QCM results clearly confirm our indirect assessments made earlier using either XRR/ellipsometry or nanoparticles adsorption.¹²⁻¹³ It is furthermore quite reassuring that those three different approaches based on different physical grounds are indeed giving the same results.

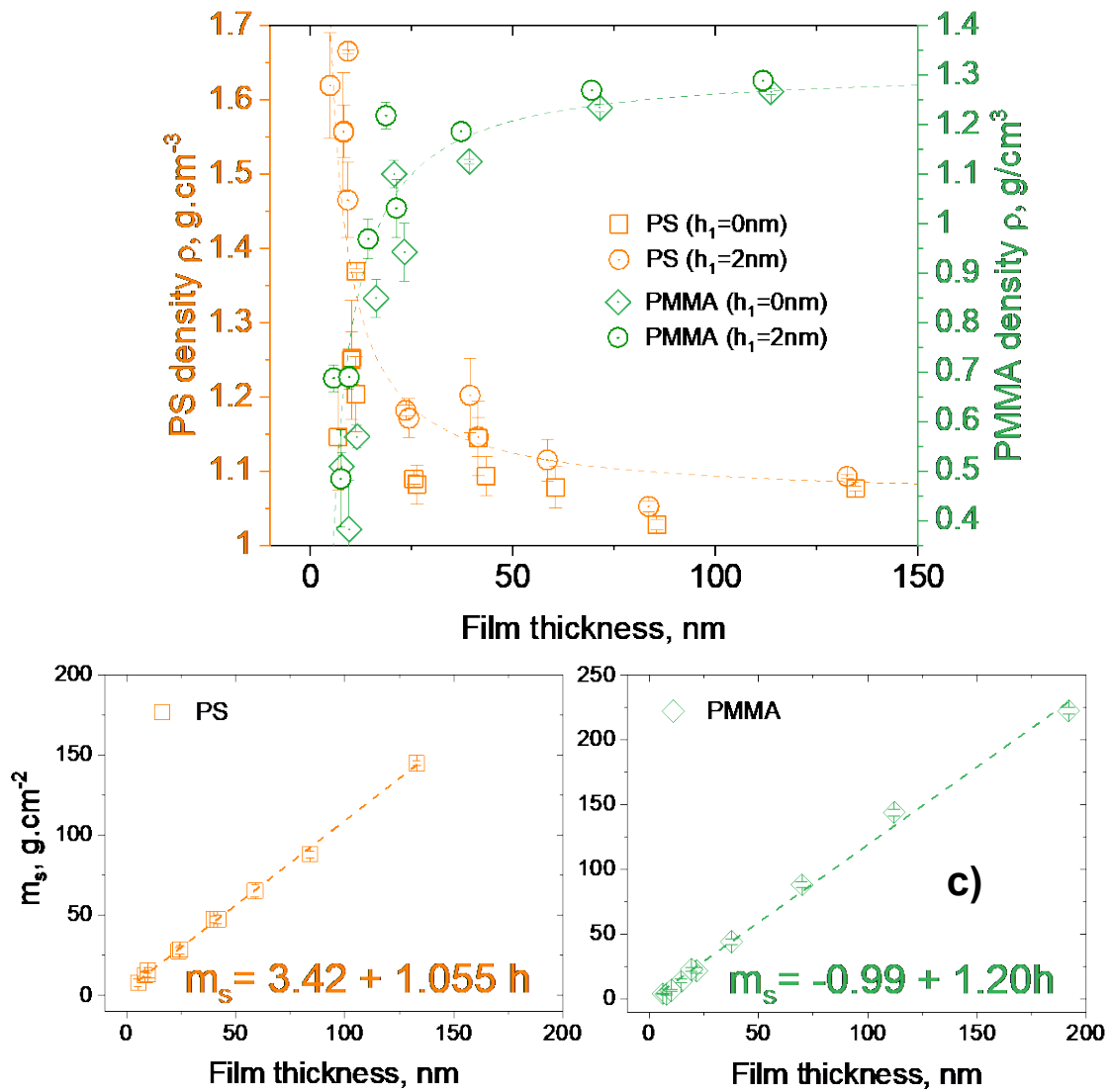


Figure 4. a) Mass density of PS (orange) and PMMA (green) ultrathin films as a function of the thickness extracted from QCM measurements. The dashed lines are a hyperbolic fit to the data (Eq. 6 and 7). b) and c) Mass per unit area m_s as a function of PS and PMMA film thickness, respectively. The dashed lines are a linear fit to the data.

The data of Figure 4a) tend to show a hyperbolic variation of the mass density with the PS film thickness according to

$$\rho(PS) = \frac{K}{h} + \rho_{bulk} \quad [6]$$

$$\rho(PMMA) = \rho_{bulk} - \frac{K}{h} \quad [7]$$

It follows that m_s should then increase linearly according to

$$m_s(PS) = \rho(h)h = K + \rho_{bulk}h \quad [8]$$

$$m_s(PMMA) = \rho(h)h = \rho_{bulk}h - K \quad [9]$$

Figure 4b) and c) clearly confirms this statement where m_s shows a linear variation with a slope of 1.055 and 1.20 g/cm³ corresponding well to the bulk mass density of PS and PMMA respectively.⁵³ Our initial assumption of a hyperbolic variation of the density with the film thickness is then experimentally confirmed.

If we consider the absolute value of the mass density, it can be challenging for the thinnest PS films where ρ lies between 1.36 and 1.66 g/m³. Such a value might appear unphysical if one thinks about the bulk conformation of polymer chains (with no interaction with any interface) where the amorphous state cannot have a higher density than its crystalline counterpart. Furthermore, if one considers the Van der Waals volume of a styrene monomer (66.1 cm³/mol) and its molecular weight (~ 105 g/mol), it follows a monomer density of 1.59 g/cm³. A close-packing of these “monomers” in 3D although unusual would give a density of (0.74 * 1.59) ~ 1.17 g/cm³. A calculation that does not take in account any extra interaction coming into play at the polymer/substrate interface. Within ultra-thin supported polymer films, the chains might indeed be strongly attracted to the surface leading to some densification/stratification²⁵. Indeed, it appears from recent simulation and experimental reports that very high density well above the bulk values can be obtained in PS (/PMMA) films either under strong confinement⁵⁴⁻⁵⁵

or high pressure.⁵⁵⁻⁵⁶ Rissannou and Harmandaris have simulated that a PS film supported by multiple graphene sheets would have a maximum density peak at 5 g/cm^3 very close to the substrate⁵⁴ with an almost parallel orientation of the phenyl with respect to the graphene surface. Of course, silicon is not graphene but the interactions unfolding at the PS/silicon interface are significant otherwise there would not be the presence of a residual and irreversibly adsorbed polymer layer.^{35, 42-43} It should be noted that a strong increase of the density close to the substrate is not incompatible with an increase of mobility at the free surface. In the same study, Rissanou and Harmandaris⁵⁴ have shown that the phenyl rings actually extend into the air in an almost perpendicular orientation with, apparently, a much faster mobility of the PS chains. What is important in this work is the trend line of the variation of the density as a function of the film thickness rather than its absolute value, which may indeed be very sensitive to the final thickness of the residual layer. The QCM methodology allows direct measurement of the upper and lower density limits for a given residual layer thickness.

This peculiar increase of the PS film density might be due, as pointed out further up, to a confinement effect which directly impacts the chain conformation.⁵⁻⁶ Jones *et al.*⁵ have used Small-Angle Neutron Scattering (SANS) to probe the molecular conformation of PS chains in ultrathin and confined films. The authors have shown that the chains retain their unperturbed Gaussian conformations in the direction parallel to the surface of the film whereas the radius of gyration of the chains in the confinement direction is strongly reduced. Based on these results, one might expect that such a conformation would favor denser films. In a similar vein, Koga *et al.*^{22, 57} have shown by X-ray and neutron reflectivity experiments that an adsorbed PS layer at the

polymer/substrate interface are composed of two different sublayers: i) flattened chains in contact with the substrate with higher density than bulk (compact chain packing) and ii) loosely adsorbed chains with bulk density in contact with air.

Furthermore, to explain the opposite trend observed for the PMMA i.e the decrease of the film density with the thickness (figure 4b), we can hypothesize that the polymer chain conformation at the polymer/SiO₂ interface play a key role.⁵⁸⁻⁵⁹ PMMA chains at such hydrophilic interface exhibit oriented methyl ester groups along the direction normal to the interface⁶⁰ reducing then the number of available conformations. These restrictions may lead to situations where larger segments of the chains can no longer arrange themselves in a denser way as in the bulk. **At this point, it should be noted that our atactic PMMA has no reason to exhibit higher density at the substrate interface, as recently shown by Ahn *et al.*⁶¹ by X-ray reflectivity; a feature usually observed with stereoregular PMMA.⁶²**

In addition to the role played by the chain conformation, another point that could be considered is the amount of solvent sequestered in the films after annealing. Because vitrification of spincoated films generally occurs during solvent removal, it was pointed out that residual solvent can remain trapped inside the thin films⁶³ thus increasing definitively the average density of the films. The study of Garcia-Turiel and Jérôme using gas chromatography showed that the relative amount of trapped toluene located at the PS–substrate interface increased from 2 to ~35% with decreasing thickness from 500 to 15 nm.⁶⁴ Although reported by others groups⁶⁵⁻⁶⁶, such enrichment effect is still far from being unanimously accepted.⁶⁷ Regarding PMMA films, there are not enough extensive studies to identify a clear trend. However, it is

conceivable that in the case of a lower density the solvent can be removed more easily upon annealing.

Correlation between Tg and mass density in thin films

Such a variation of the density in ultra-thin PMMA and PS films naturally raises the following question: *Are the reduction in film thickness and the subsequent increase/decrease in the mass density compatible with a depression/rise of the Tg as commonly reported in the literature for PS⁶⁸ and PMMA⁶⁹⁻⁷⁰ respectively?* Indeed, the Tg reduction observed for PS ultra-thin films and ascribed to an increase in the free volume seems rather contradictory with a higher mass density. In fact, we believe that the argument that states that PS ultra-thin films should have more free volume **at room temperature** (RT) than in the bulk is likely misleading. In fact, the value of the film density at room temperature (about 20°C) is in no way predictive of its variation with temperature; or how the polymer film will gain free volume with temperature as well. One crucial parameter to take into account is the coefficient of thermal expansion (CTE) which refers to the rate at which a material expands with an increase in temperature. Especially, for PS films, several papers^{45, 68, 71} reported an increase of the CTE with decreasing thickness.

In order to better understand the role played by the CTE in this context, we have monitored the thermal expansion of PMMA and PS thin films as a function of their thicknesses with the help of temperature-controlled hot stage ellipsometer. The measured values are gathered in table 3 and shown in the Figure 6 together with data coming from previous literature results.^{44, 68, 71} It is observed that Tg increases (table

3) with decreasing PMMA film thickness, while CTE dramatically decreases in the glassy state as the film thickness is reduced below 50 nm.

	PMMA										PS		
Thickness (nm)	5	7	10	15	20	30	60	100	160	13	26	83	
T _g (°C)	125	120	125	125	105	115	115	115	115	78	88	99	
CTE 10 ⁻⁴ K	0.68	1.12	1.38	1.49	1.53	1.59	1.66	2.35	2.28	6.9	4.9	2.3	

Table 3. Glass transition temperature (T_g) and coefficient of thermal expansion (CTE) of PMMA and PS¹³ thin films in the glassy state as a function of their thickness.

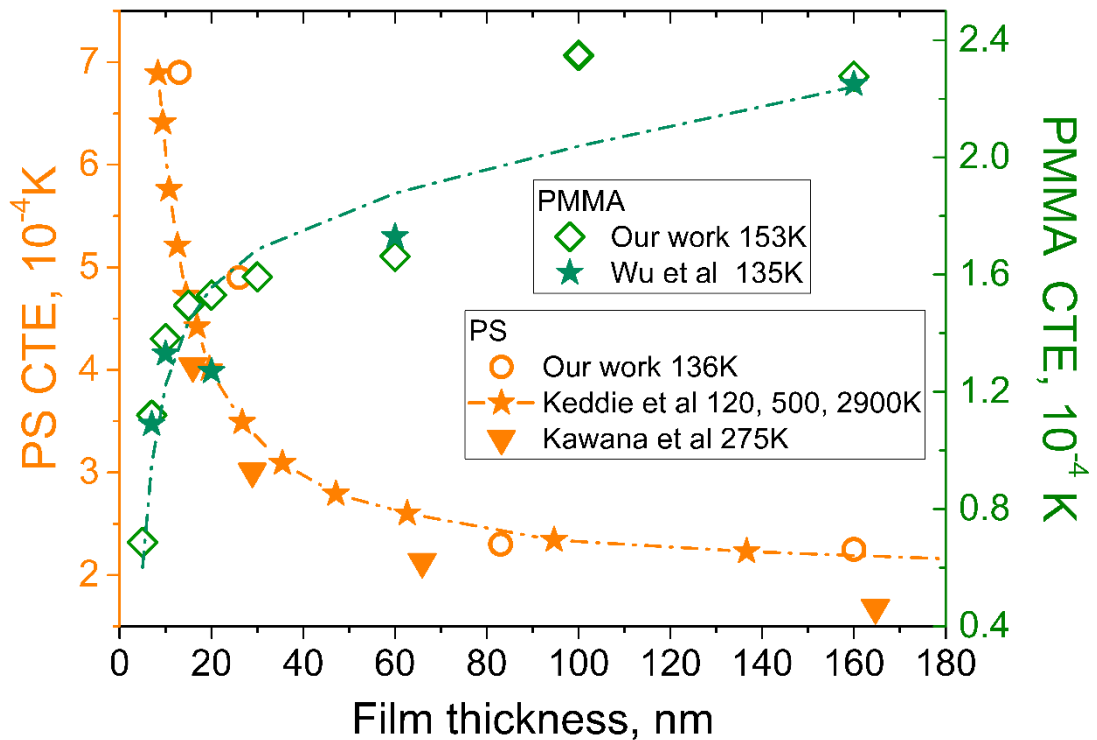


Figure 5. Thermal expansivity of PS and PMMA films supported on SiO_x-Si⁴⁴ and H-Si^{45, 68} surfaces, measured in the glassy state by ellipsometry^{45, 68} and neutron reflectivity.⁴⁴

It is striking to observe that the variation of CTE with the film thickness seems opposite for PMMA and PS as in the case of the mass density and T_g (Figure 5). From these results, it is then clear that if thinner PS films thermally expand more rapidly than thicker ones, they may reach the critical free volume at a lower temperature (T_g). **In other words, the thinnest film reaches the critical density (inverse of the critical free volume) before the thick film (see Figure S6).** An analogy could be made between the behavior of an ultrathin PS film and that of a spring which, once compressed, has stored potential energy. The energy inside the film originating from confinement effects when the thickness is reduced and the interfacial interactions with the two interfaces would be released by a thermal energy input or by the influence of a supercritical gas. As an example, ultra-thin PS films show abnormal high swelling under supercritical CO₂ (70% versus 5% in bulk).⁷²⁻⁷³ As ellipsometry does not directly measure the free volume, we have extracted (Figure 6) from the work of Ougizawa *et al.*⁷⁴ free volume variations of PS (1090K) thin films on silicon wafers for two thicknesses (22 and 1200 nm) studied by energy variable positron annihilation lifetime spectroscopy (EVPALS). From Figure 6a, one can draw the following conclusions: (i) the free volume (hence **the inverse of the density**) at RT is smaller in the 22 nm thin film than in 1200 nm bulky one (ii) the free volume in the 22 nm thick film increases with temperature much faster than for the 1200 nm bulky film, in perfect agreement with our ellipsometric results (Fig.6). (iii) the T_g associated with the free volume variation is 84 and 100 °C for 22 nm and 1200 nm films, respectively.

The thermal expansion coefficient is found to increase sharply as film thickness is decreased. This behavior is obtained both in the glassy and rubbery states. This dependence of the CTE on the thickness of the film in the melt has already been highlighted by other authors,^{21, 71} and could be explained by (i) the interactions unfolding at the substrate/ PS film that influence its behavior below and above T_g .⁷⁵ (ii) fast evaporation of the solvent during the spin-coating process that can lead to non-equilibrium conformations of the polymer chains. As a result, the chains are trapped in distorted conformations with a reduced degree of interchain overlap introducing residual stresses into the film. Even though residual stresses are found to fade away upon increasing annealing time and temperature, they cannot be completely suppressed.⁷⁶

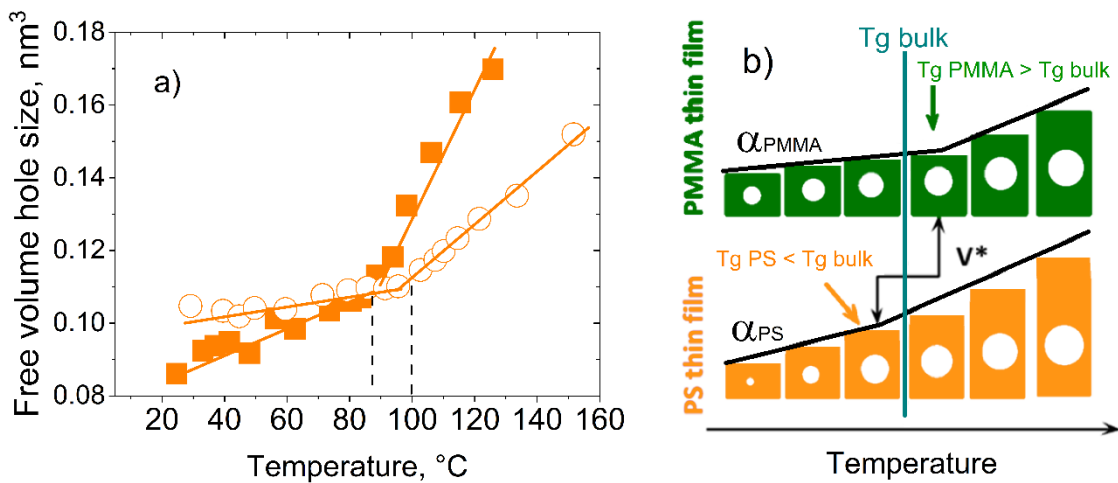


Figure 6. a) Change of free volume hole size with temperature of 22 nm (orange square) and 1200 nm (orange circle) PS films extracted from literature.⁷⁴ b) Schematic representation showing that the critical free volume V^* is reached at a lower

temperature for the thinner PS film and at higher temperature for the PMMA thinner film.

PMMA (and PS) thin films are known to have higher and lower T_g respectively than in the bulk. It is then conceivable to assume that T_g is higher (/lower) because such thin films reach their critical free volume at a higher (/lower) temperature due to a lower(/higher) thermal expansion as schematically depicted in figure 6b.

CONCLUSION

Understanding how mass density varies in polymer thin films is not an easy task because many measurement techniques rely heavily on modeling, and thus are not applicable to thin films for which the density may not be homogeneous due to the presence of interfaces. In this work, we proposed a new approach to *directly measure* the mass density of thin and ultrathin polymer films by monitoring their dissolution in good solvent in a QCM cell through the systematic measurement of the overall mass loss as a function of their thickness. This method does not require any intermediate quantity such as the refractive index nor any particular model to analyze the data to get insights on the polymer film mass density. In a first part, we have validated our methodology by measuring densities of three common thick (>100nm) glassy polymers films with values very similar to those reported in the literature. In a second part, we tackled to measure the mass density variation of ultra-thin PS and PMMA films with thickness. The results showed an opposite behavior for PS and PMMA. These striking results raised the question of the consistency of an increase/decrease in mass density with the commonly observed depression/elevation of T_g for PS and PMMA films.

Although there is still some uncertainty in the absolute value of the density of ultrathin films due to imprecision in the thickness the residual layer, the QCM dissolution technique allows to delimit its borders. Beyond that, it is worth to note that our direct measurements are in very good agreement with many other works in the literature based on different physical grounds (e.g., ellipsometry^{13, 21}, x-ray reflectivity^{13, 21}, EVPALS⁷⁴, contact angle measurement²⁹, characterization of nanoparticles adsorption¹², magnetic Levitation^{51, 77}) leading to a large experimental consensus on the variation of the mass density of ultrathin PS films with thickness.

In the last part, we have measured the thermal expansion of both polymers to better understand the role of the **coefficient of thermal expansion** in the peculiar properties of these thin films. Surprisingly, the **coefficient of thermal expansion** CTE and the mass density showed a similar variation with thickness, pointing out a clear correlation between the glass transition temperature, the coefficient of thermal expansion and the free volume of the polymer thin films. This key result finally enables to rationalize the counter-intuitive and opposite variation between the mass density and the T_g found in this work for both PMMA and PS thin films; an interpretation that is not incompatible with the role played by other features like an increased chain mobility at the free surface of a PS film for example. It is important to note that this apparent link between CTE, density and T_g, highlighted in this work on two polymers, needs to be further investigated to test its soundness before generalizing it. The effect of the interactions unfolding at the substrate/film interface on CTE and T_g is currently under investigation.

ACKNOWLEDGMENT

The authors acknowledge the regions of Bretagne and Pays de la Loire and the French National Research Agency (SISAL project ANR-18-CE06-0016) for their financial support.

REFERENCES

1. Ediger, M.; Forrest, J., Dynamics near free surfaces and the glass transition in thin polymer films: a view to the future. *Macromolecules* **2014**, *47* (2), 471-478.
2. Kremer, F.; Tress, M.; Mapesa, E. U., Glassy dynamics and glass transition in nanometric layers and films: A silver lining on the horizon. *Journal of Non-Crystalline Solids* **2015**, *407*, 277-283.
3. Napolitano, S.; Glynos, E.; Tito, N. B., Glass transition of polymers in bulk, confined geometries, and near interfaces. *Reports on Progress in Physics* **2017**, *80* (3), 036602.
4. Russell, T. P.; Chai, Y., 50th anniversary perspective: Putting the squeeze on polymers: A perspective on polymer thin films and interfaces. *Macromolecules* **2017**, *50* (12), 4597-4609.
5. Jones, R. L.; Kumar, S. K.; Ho, D. L.; Briber, R. M.; Russell, T. P., Chain conformation in ultrathin polymer films. *Nature* **1999**, *400* (6740), 146-149.
6. Kraus, J.; Müller-Buschbaum, P.; Kuhlmann, T.; Schubert, D.; Stamm, M., Confinement effects on the chain conformation in thin polymer films. *EPL (Europhysics Letters)* **2000**, *49* (2), 210.
7. Mansfield, K. F.; Theodorou, D. N., Molecular dynamics simulation of a glassy polymer surface. *Macromolecules* **1991**, *24* (23), 6283-6294.
8. Fakhraai, Z.; Forrest, J. A., Probing slow dynamics in supported thin polymer films. *Physical review letters* **2005**, *95* (2), 025701.
9. Reiter, G., Mobility of polymers in films thinner than their unperturbed size. *EPL (Europhysics Letters)* **1993**, *23* (8), 579.
10. Reiter, G., Dewetting as a probe of polymer mobility in thin films. *Macromolecules* **1994**, *27* (11), 3046-3052.
11. Yang, Z.; Fujii, Y.; Lee, F. K.; Lam, C.-H.; Tsui, O. K., Glass transition dynamics and surface layer mobility in unentangled polystyrene films. *Science* **2010**, *328* (5986), 1676-1679.
12. Unni, A. B.; Vignaud, G.; Chapel, J.; Giermanska, J.; Bal, J.; Delorme, N.; Beuvier, T.; Thomas, S.; Grohens, Y.; Gibaud, A., Probing the density variation of confined polymer thin films via simple model-independent nanoparticle adsorption. *Macromolecules* **2017**, *50* (3), 1027-1036.
13. Vignaud, G.; S. Chebil, M.; Bal, J.; Delorme, N.; Beuvier, T.; Grohens, Y.; Gibaud, A., Densification and depression in glass transition temperature in polystyrene thin films. *Langmuir* **2014**, *30* (39), 11599-11608.
14. Bal, J.; Beuvier, T.; Chebil, M.; Vignaud, G.; Grohens, Y.; Sanyal, M.; Gibaud, A., Relaxation of ultrathin polystyrene films Hyperswollen in supercritical carbon dioxide. *Macromolecules* **2014**, *47* (24), 8738-8747.
15. Cangialosi, D.; Boucher, V. M.; Alegría, A.; Colmenero, J., Direct evidence of two equilibration mechanisms in glassy polymers. *Physical review letters* **2013**, *111* (9), 095701.
16. Forrest, J. A.; Mattsson, J., Reductions of the glass transition temperature in thin polymer films: Probing the length scale of cooperative dynamics. *Physical review E* **2000**, *61* (1), R53.
17. McCoy, J. D.; Curro, J. G., Conjectures on the glass transition of polymers in confined geometries. *The Journal of chemical physics* **2002**, *116* (21), 9154-9157.
18. White, R. P.; Lipson, J. E., Polymer free volume and its connection to the glass transition. *Macromolecules* **2016**, *49* (11), 3987-4007.
19. White, R. P.; Lipson, J. E., Free volume in the melt and how it correlates with experimental glass transition temperatures: results for a large set of polymers. *ACS Macro Letters* **2015**, *4* (5), 588-592.

20. Wallace, W.; Beck Tan, N.; Wu, W.; Satija, S., Mass density of polystyrene thin films measured by twin neutron reflectivity. *The Journal of chemical physics* **1998**, *108* (9), 3798-3804.
21. Ata, S.; Kuboyama, K.; Ito, K.; Kobayashi, Y.; Ougizawa, T., Anisotropy and densification of polymer ultrathin films as seen by multi-angle ellipsometry and X-ray reflectometry. *Polymer* **2012**, *53* (4), 1028-1033.
22. Gin, P.; Jiang, N.; Liang, C.; Taniguchi, T.; Akgun, B.; Satija, S. K.; Endoh, M. K.; Koga, T., Revealed architectures of adsorbed polymer chains at solid-polymer melt interfaces. *Physical review letters* **2012**, *109* (26), 265501.
23. Pradipkanti, L.; Chowdhury, M.; Satapathy, D. K., Stratification and two glass-like thermal transitions in aged polymer films. *Physical Chemistry Chemical Physics* **2017**, *19* (43), 29263-29270.
24. Reiter, G.; Napolitano, S., Possible origin of thickness-dependent deviations from bulk properties of thin polymer films. *Journal of Polymer Science Part B: Polymer Physics* **2010**, *48* (24), 2544-2547.
25. Bollinne, C.; Stone, V.; Carlier, V.; Jonas, A. M., Density perturbations in polymers near a solid substrate: An X-ray reflectivity study. *Macromolecules* **1999**, *32* (14), 4719-4724.
26. Pershan, P. S., X-ray or neutron reflectivity: limitations in the determination of interfacial profiles. *Physical Review E* **1994**, *50* (3), 2369.
27. Vignaud, G.; Gibaud, A., REFLEX: a program for the analysis of specular X-ray and neutron reflectivity data. *Journal of Applied Crystallography* **2019**, *52* (1), 201-213.
28. Tompkins, H.; Irene, E. A., *Handbook of ellipsometry*. William Andrew: 2005.
29. Li, Y.; Pham, J. Q.; Johnston, K. P.; Green, P. F., Contact angle of water on polystyrene thin films: Effects of CO₂ environment and film thickness. *Langmuir* **2007**, *23* (19), 9785-9793.
30. Beena Unni, A.; Vignaud, G.; Bal, J.; Delorme, N.; Beuvier, T.; Thomas, S.; Grohens, Y.; Gibaud, A., Solvent assisted rinsing: Stability/instability of ultrathin polymer residual layer. *Macromolecules* **2016**, *49* (5), 1807-1815.
31. Han, Y.; Huang, X.; Rohrbach, A. C.; Roth, C. B., Comparing refractive index and density changes with decreasing film thickness in thin supported films across different polymers. *The Journal of Chemical Physics* **2020**, *153* (4), 044902.
32. Huang, X.; Roth, C. B., Changes in the temperature-dependent specific volume of supported polystyrene films with film thickness. *The Journal of chemical physics* **2016**, *144* (23), 234903.
33. Johannsmann, D., The quartz crystal microbalance in soft matter research. *Soft and Biological Matter* **2015**, 191-204.
34. Zhang, C.; Fujii, Y.; Tanaka, K., Effect of long range interactions on the glass transition temperature of thin polystyrene films. *ACS Macro Letters* **2012**, *1* (11), 1317-1320.
35. Bal, J. K.; Beuvier, T.; Unni, A. B.; Chavez Panduro, E. A.; Vignaud, G.; Delorme, N.; Chebil, M. S.; Grohens, Y.; Gibaud, A., Stability of polymer ultrathin films (< 7 nm) made by a top-down approach. *Acs Nano* **2015**, *9* (8), 8184-8193.
36. Choi, S.-H.; Newby, B.-m. Z., Suppress polystyrene thin film dewetting by modifying substrate surface with aminopropyltriethoxysilane. *Surface science* **2006**, *600* (6), 1391-1404.
37. Xu, L.; Sharma, A.; Joo, S. W., Substrate heterogeneity induced instability and slip in polymer thin films: dewetting on silanized surfaces with variable grafting density. *Macromolecules* **2010**, *43* (18), 7759-7762.
38. Xue, L.; Han, Y., Inhibition of dewetting of thin polymer films. *Progress in Materials Science* **2012**, *57* (6), 947-979.
39. Cassiède, M.; Paillol, J.; Pauly, J.; Daridon, J.-L., Electrical behaviour of AT-cut quartz crystal resonators as a function of overtone number. *Sensors and Actuators A: Physical* **2010**, *159* (2), 174-183.
40. Kanazawa, K. K.; Gordon, J. G., Frequency of a quartz microbalance in contact with liquid. *Analytical Chemistry* **1985**, *57* (8), 1770-1771.
41. Guiselin, O., Irreversible adsorption of a concentrated polymer solution. *EPL (Europhysics Letters)* **1992**, *17* (3), 225.

42. Napolitano, S., Irreversible adsorption of polymer melts and nanoconfinement effects. *Soft Matter* **2020**.
43. Nieto Simavilla, D.; Huang, W.; Housmans, C.; Sferrazza, M.; Napolitano, S., Taming the strength of interfacial interactions via nanoconfinement. *ACS central science* **2018**, *4* (6), 755-759.
44. Wu, W.-I.; van Zanten, J. H.; Orts, W. J., Film thickness dependent thermal expansion in ultrathin poly (methyl methacrylate) films on silicon. *Macromolecules* **1995**, *28* (3), 771-774.
45. Kawana, S.; Jones, R. A., Character of the glass transition in thin supported polymer films. *Physical Review E* **2001**, *63* (2), 021501.
46. Sekar, S.; Giermanska, J.; Chapel, J.-P., Reusable and recyclable quartz crystal microbalance sensors. *Sensors and Actuators B: Chemical* **2015**, *212*, 196-199.
47. Johannsmann, D., Viscoelastic analysis of organic thin films on quartz resonators. *Macromolecular Chemistry and Physics* **1999**, *200* (3), 501-516.
48. Fujii, Y.; Yang, Z.; Leach, J.; Atarashi, H.; Tanaka, K.; Tsui, O. K., Affinity of polystyrene films to hydrogen-passivated silicon and its relevance to the T_g of the films. *Macromolecules* **2009**, *42* (19), 7418-7422.
49. Reviakine, I.; Johannsmann, D.; Richter, R. P., Hearing what you cannot see and visualizing what you hear: interpreting quartz crystal microbalance data from solvated interfaces. ACS Publications: 2011.
50. Orwoll, R. A., Densities, coefficients of thermal expansion, and compressibilities of amorphous polymers. In *Physical properties of polymers handbook*, Springer: 2007; pp 93-101.
51. Root, S.; Gao, R.; Ge, S.; Whitesides, G., Density Measurements of Thin Polymeric Films using Magnetic Levitation. *Bulletin of the American Physical Society* **2020**.
52. Rodahl, M.; Höök, F.; Fredriksson, C.; Keller, C. A.; Krozer, A.; Brzezinski, P.; Voinova, M.; Kasemo, B., Simultaneous frequency and dissipation factor QCM measurements of biomolecular adsorption and cell adhesion. *Faraday discussions* **1997**, *107*, 229-246.
53. Kasarova, S. N.; Sultanova, N. G.; Ivanov, C. D.; Nikolov, I. D., Analysis of the dispersion of optical plastic materials. *Optical Materials* **2007**, *29*, 1481-1490.
54. Rissanou, A. N.; Harmandaris, V., Structural and dynamical properties of polystyrene thin films supported by multiple graphene layers. *Macromolecules* **2015**, *48* (8), 2761-2772.
55. Wei, X.; Luo, T., Role of Ionization in Thermal Transport of Solid Polyelectrolytes. *The Journal of Physical Chemistry C* **2019**, *123* (20), 12659-12665.
56. Hsieh, W.-P.; Losego, M. D.; Braun, P. V.; Shenogin, S.; Keblinski, P.; Cahill, D. G., Testing the minimum thermal conductivity model for amorphous polymers using high pressure. *Physical Review B* **2011**, *83* (17), 174205.
57. Barkley, D. A.; Jiang, N.; Sen, M.; Endoh, M. K.; Rudick, J. G.; Koga, T.; Zhang, Y.; Gang, O.; Yuan, G.; Satija, S. K., Chain conformation near the buried interface in nanoparticle-stabilized polymer thin films. *Macromolecules* **2017**, *50* (19), 7657-7665.
58. Chandran, S.; Baschnagel, J. r.; Cangialosi, D.; Fukao, K.; Glynos, E.; Janssen, L. M.; Müller, M.; Muthukumar, M.; Steiner, U.; Xu, J., Processing pathways decide polymer properties at the molecular level. *Macromolecules* **2019**, *52* (19), 7146-7156.
59. Zuo, B.; Zhou, H.; Davis, M. J.; Wang, X.; Priestley, R. D., Effect of Local Chain Conformation in Adsorbed Nanolayers on Confined Polymer Molecular Mobility. *Physical review letters* **2019**, *122* (21), 217801.
60. Inutsuka, M.; Horinouchi, A.; Tanaka, K., Aggregation states of polymers at hydrophobic and hydrophilic solid interfaces. *ACS Macro Letters* **2015**, *4* (10), 1174-1178.
61. Ahn, S. I.; Kim, J.-H.; Kim, J. H.; Jung, J. C.; Chang, T.; Ree, M.; Zin, W.-C., Polarity effect near the surface and interface of thin supported polymer films: X-ray reflectivity study. *Langmuir* **2009**, *25* (10), 5667-5673.
62. Van der Lee, A.; Hamon, L.; Holl, Y.; Grohens, Y., Density profiles in thin PMMA supported films investigated by X-ray reflectometry. *Langmuir* **2001**, *17* (24), 7664-7669.

63. Tsige, M.; Grest, G. S., Solvent evaporation and interdiffusion in polymer films. *Journal of Physics: Condensed Matter* **2005**, *17* (49), S4119.
64. García-Turiel, J.; Jérôme, B., Solvent retention in thin polymer films studied by gas chromatography. *Colloid and polymer science* **2007**, *285* (14), 1617-1623.
65. Perlich, J.; Metwalli, E.; Schulz, L.; Georgii, R.; Müller-Buschbaum, P., Solvent content in thin spin-coated polystyrene homopolymer films. *Macromolecules* **2009**, *42* (1), 337-344.
66. Zhang, X.; Berry, B. C.; Yager, K. G.; Kim, S.; Jones, R. L.; Satija, S.; Pickel, D. L.; Douglas, J. F.; Karim, A., Surface morphology diagram for cylinder-forming block copolymer thin films. *ACS Nano* **2008**, *2* (11), 2331-2341.
67. Zhang, X.; Yager, K. G.; Kang, S.; Fredin, N. J.; Akgun, B.; Satija, S.; Douglas, J. F.; Karim, A.; Jones, R. L., Solvent retention in thin spin-coated polystyrene and poly (methyl methacrylate) homopolymer films studied by neutron reflectometry. *Macromolecules* **2010**, *43* (2), 1117-1123.
68. Keddie, J. L.; Jones, R. A.; Cory, R. A., Size-dependent depression of the glass transition temperature in polymer films. *EPL (Europhysics Letters)* **1994**, *27* (1), 59.
69. Keddie, J. L.; Jones, R. A. L.; Cory, R. A., Interface and surface effects on the glass-transition temperature in thin polymer films. *Faraday Discussions* **1994**, *98*, 219-230.
70. Lan, T.; Torkelson, J. M., Methacrylate-based polymer films useful in lithographic applications exhibit different glass transition temperature-confinement effects at high and low molecular weight. *Polymer* **2014**, *55* (5), 1249-1258.
71. Singh, L.; Ludovice, P. J.; Henderson, C. L., Influence of molecular weight and film thickness on the glass transition temperature and coefficient of thermal expansion of supported ultrathin polymer films. *Thin solid films* **2004**, *449* (1-2), 231-241.
72. Koga, T.; Seo, Y.-S.; Shin, K.; Zhang, Y.; Rafailovich, M.; Sokolov, J.; Chu, B.; Satija, S., The role of elasticity in the anomalous swelling of polymer thin films in density fluctuating supercritical fluids. *Macromolecules* **2003**, *36* (14), 5236-5243.
73. Chebil, M. S.; Vignaud, G.; Grohens, Y.; Konovalov, O.; Sanyal, M.; Beuvier, T.; Gibaud, A., In situ X-ray reflectivity study of polystyrene ultrathin films swollen in carbon dioxide. *Macromolecules* **2012**, *45* (16), 6611-6617.
74. Ata, S.; Muramatsu, M.; Takeda, J.; Ohdaira, T.; Suzuki, R.; Ito, K.; Kobayashi, Y.; Ougizawa, T., Free volume behavior in spincoated thin film of polystyrene by energy variable positron annihilation lifetime spectroscopy. *Polymer* **2009**, *50* (14), 3343-3346.
75. Pochan, D. J.; Lin, E. K.; Satija, S. K.; Wu, W.-l., Thermal expansion of supported thin polymer films: A direct comparison of free surface vs total confinement. *Macromolecules* **2001**, *34* (9), 3041-3045.
76. Reiter, G.; Hamieh, M.; Damman, P.; Sclavons, S.; Gabriele, S.; Vilmin, T.; Raphaël, E., Residual stresses in thin polymer films cause rupture and dominate early stages of dewetting. *Nature materials* **2005**, *4* (10), 754-758.
77. Root, S.; Whitesides, G.; Gao, R., Density Measurements of Thin Films of Polymers with Magnetic Levitation. *2020 Virtual AIChE Annual Meeting* **2020**.